ABSTRACT

Title of Thesis: Expansion of Polyurethane Foam in Low Pressure Environment for Space Debris Removal Applications

Team JUNK: Edward Cai, Ethan Green, Aravind Kavuturu, Finnegan O'Neill, Joseph Shedleski, John Yang, Robert J. Young, & Muhamad Zakaria

Thesis Directed By: Dr. Raymond Sedwick
Department of Aerospace Engineering

As the privatization of space flight has led to an increased number of rocket launches and a new era of space exploration, the issue of space debris is becoming a well-researched phenomenon. With more emphasis on future extraterrestrial missions, such as NASA's Artemis and SpaceX's Mars missions, there is a growing concern surrounding the unsustainable practices that create space debris. Although there is a plethora of papers discussing the sources of space debris, as well as its negative impacts on the future of space flight, there are comparatively fewer papers discussing active debris removal methods. This study focuses on one such method - namely, using spray foam to remediate space debris. Spray foam has the advantage of being low-cost and multi-use, which differs from most other active removal methods. To determine the viability of spray foam in space debris removal, this study tests the expansion of polyurethane foam in vacuum, a poorly documented characteristic in current literature. From a sample of 20 tests, a maximum volumetric expansion ratio of 53 was found. The resulting discussion focuses on spray foam's efficacy as an active debris removal method from these observations.

Expansion of Polyurethane Foam in Low Pressure Environment for Space Debris Removal Applications

Team JUNK

Edward Cai, Ethan Green, Aravind Kavuturu, Finnegan O'Neill,
Joseph Shedleski, John Yang, Robert J. Young, and Muhamad Zakaria

Thesis submitted in partial fulfillment of the requirements of the
Gemstone Honors Program, University of Maryland, 2023

Advisory Committee:
Dr. Raymond Sedwick, Advisor

Acknowledgements

The team would like to firstly thank Dr. Raymond Sedwick for his mentorship and lab provisions throughout the research and experimentation process. The team would also like to thank Ms. Jodi Coalter for her librarian assistance. For their time and insight at the Gemstone Thesis Conference, the team thanks discussants Dr. John Crassidis, Dr. Steve Mork, Dr. Gordon Roesler, and Dr. Jarred Young. Finally, the team thanks Dr. David Lovell and Dr. Allison Lansverk for their planning and organization of the Gemstone research program and the Thesis Conference, and making this research opportunity possible.

TABLE OF CONTENTS

1 INTRODUCTION

By the end of the century, space debris could be the greatest hazard for space exploration. An increasingly privatized space industry has led to more interest in rocket launches in recent decades, and the result is an ever-growing number of objects in Earth's orbit. To that end, there has been an increased focus on space debris in recent literature - the causes, sizes, and impacts of space debris are well documented. Although there is a greater awareness for this emerging threat, there has been comparatively little done to remove space debris. The currently proposed technologies are slow to be adopted, and though the field of active debris removal has many options, there have been no major efforts on the part of space agencies or governments to employ one of these methods to clean up space debris.

Space debris is defined as any man-made object currently in orbit around Earth that no longer serves a purpose. The various forms of space debris include, but are not limited to, decommissioned spacecraft and payloads, spent rocket stages, collisional debris, and debris from unidentified sources. From a European Space Agency (ESA) estimate for 2022, there are approximately 30,000 pieces of space debris currently being tracked, ranging in size and altitude, in Earth's atmosphere today [4]. The number of objects from each source is shown in Figure 1 below.

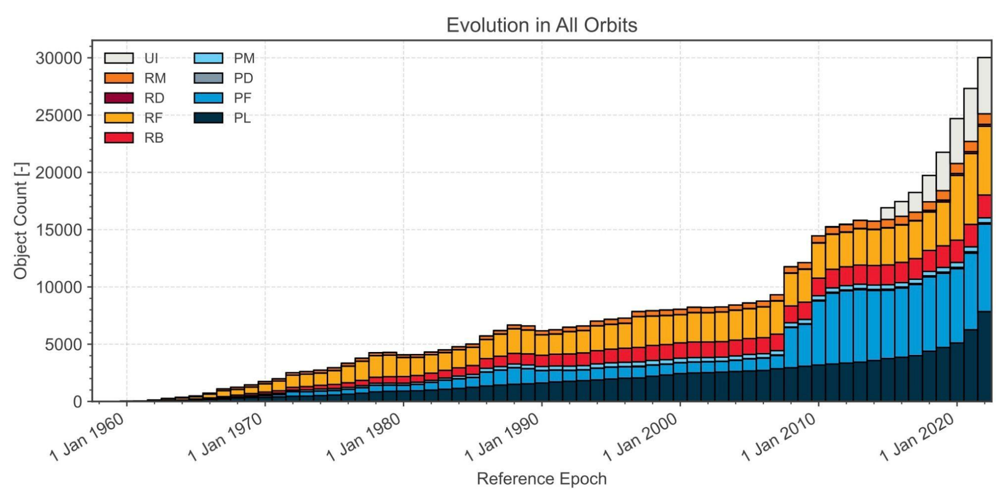

Figure 1: Graph of orbital debris from 1960 to 2020, separated by source.

UI - unidentified, RM - rocket mission related object, RD - rocket debris, RF - rocket fragmentation debris, RB - rocket body, PM - payload mission related object, PD - payload debris, PF - payload fragmentation debris, PL - payload.

From the graph, the most common form of debris is in the form of unidentified debris, with rocket-related debris and payload-related debris following. Although there are about 30,000 pieces being tracked, the total number of objects is estimated to be over 100 million, with the bulk ranging from 1mm to 10cm [4].

The time-sensitive nature of the space debris problem comes from collisional cascading, a positive feedback loop where the presence of space debris increases the likelihood of collisions and fragmentation, which increases the amount of space debris. The positive feedback loop of collisional cascading is known as the Kessler Syndrome, which was first formally named after Donald J. Kessler [2]. In this paper, Kessler presented a mathematical model for predicting when collisional cascading would reach critical mass - at this point, even if no more space objects were introduced into orbit, the amount of space debris would continue to grow indefinitely. The original prediction for the "critical mass date" was approximately 2010-2020.

In considering methods of handling space debris, there are active and passive methods. Active debris removal methods are primarily focused on removing larger, trackable debris due to the inability to efficiently remove smaller debris [16]. Thus, active debris methods are more widely studied, as there are more efficient options to deorbit large debris. There have been many proposed methods of active debris removal, with only a few discussed here. Net capture involves the use of a net to drag debris down to deorbit with a leading satellite, tether or harpoon removal involves directly penetrating the debris with a satellite in order to deorbit, and laser-based ablation ionizes the surface of debris to cause a slight thrust down towards Earth, deorbiting. All three methods listed here have been studied extensively, but the focus of this study is on a less popular method: spray foam.

In using spray foam, the leading satellite can carry a large volume of liquid reagents that can combine to form foam on the debris. By increasing the mass-to-area ratio, the foam allows the debris to deorbit itself, without the need for physical contact. By using foams with high expansion ratios, the deployment satellite can be highly reusable and could feasibly deorbit many hundreds of debris objects before becoming non-operational. However, this method requires the satellite to deploy foam directly onto the surface of debris, requiring high precision for either aiming foam reagents from a distance or manipulating an exterior arm for direct deployment. In either case, the deployment system for spray foam is a topic for further study and refinement. In this study, the basic expansion characteristics of foam are tested in order to determine if spray foam can conceivably deorbit space debris.

The use of spray foam is a relatively novel field of research. Studies into dynamic simulations of deorbiting debris with spray foam are widespread, along with the characteristics of different foams. However, there is little practical research into the expansion characteristics of foam in vacuum conditions. Some studies have modeled the expansion theoretically, but very few experimental studies are available to verify these results.

2 LITERATURE REVIEW

2.1 Introduction to Foam-Based Removal Methods

Foam-based removal methods involve a spacecraft that deploys expandable foam on the surface of orbital debris, which when activated, significantly increases the debris' surface area, inducing more atmospheric drag and eventually causing the target to deorbit. Most of the research into this method stems from a singular source — a lengthy report presented to the ESA in 2011 detailing the chemistry, effectiveness, and feasibility of a foam removal method [10]. The report proposed the foam to be sprayed from a gun or a nozzle from a single spacecraft or a potential satellite swarm. Specific types of foam, from glass to polymer-based, were researched, and computer simulations modeled the expansion behavior of polymer-based foams.

While the idea is novel and untested, the study found numerous potential advantages. First, this method could be tailored to remove various sizes and masses of LEO debris based on the quantity of foam deployed. Second, there would be no necessity to control the target debris after deployment — the debris would simply make an uncontrolled reentry and disintegrate in the Earth's atmosphere.

There are certainly disadvantages to this method as well - since the method relies on aerodynamic drag, it is most effective for LEO debris. Large debris located in higher orbits would take significantly longer to deorbit or be unable to be deorbited at all. The relative lack of research into this method compared to other proposed methods indicates a low technology readiness level, implying that such a method would have significant development hurdles to overcome in testing and validation to be spaceworthy.

2.2 Proposed Deployment Techniques

An essential element in the foam debris removal process is the method of deploying the foam. Optimally, foam will be deployed in such a manner that it will surround the debris as shown in Fig. 4.

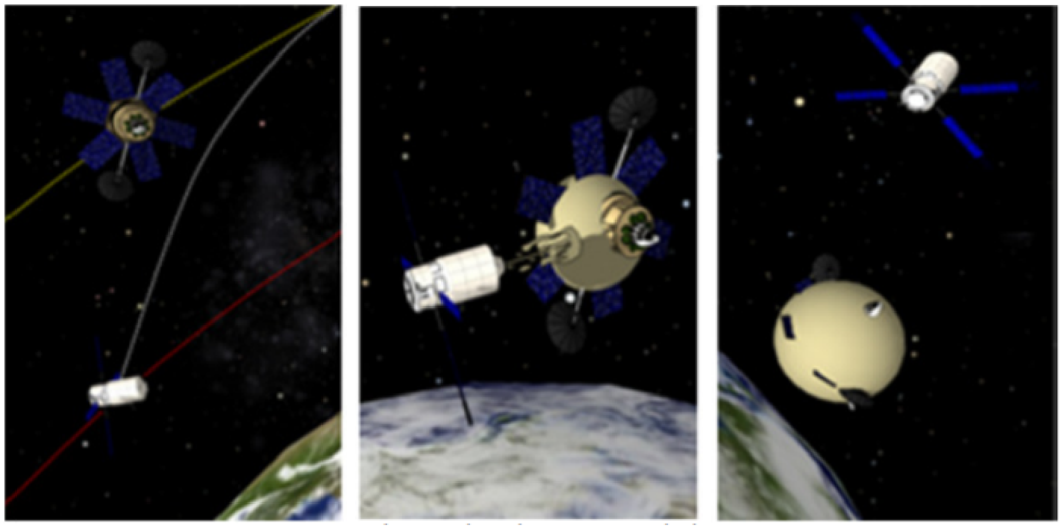

a. b. c.

Figure 4: (a) The rendezvous with debris, (b) the beginning of foam deployment, (c) separation and de-orbiting of debris [10].

Based on previous work on the subject, four main methodologies for the deployment of foam onto orbital debris were identified [10]:

Chameleon Tongue

The spacecraft approaches a piece of debris. A retractable-wire extends from the spacecraft, with the reservoirs storing the foam components and the mixing chamber that catalyzes the reaction attached to the extended end. Once the wire reaches the debris, the foam chamber is placed on the debris and the wire retracts back to the spacecraft. The mixing chamber then catalyzes the reaction, enveloping the debris in the created foam.

One of the main concerns with this method is its lack of development. Retractable tether, active reaction deployment device, and foam catalyzing chamber technologies all exist independently, with no collective design of the system. Furthermore, the foam chamber must also adhere to the debris while foaming. This could pose a problem if the foam chamber detaches from the debris during the reaction process. Smaller debris introduce complications, as generally, they have higher velocities and are more prone to rotation which would make it more difficult to place the chamber on the debris. Finally, this method has the same drawbacks as many tether technologies —it requires precise data on the debris' position, velocity, and rotation.

Foam Ejection Nozzle

This method consists of a nozzle attached to a robotic arm, which ejects foam onto the debris face. The length of this arm depends on the radius of the ball of foam surrounding the debris. If the spacecraft is too close to the debris, there is a chance that the foam might attach to the spacecraft, so a robotic arm with a length of 15 m is a conservative estimate for a foamed debris with a maximum radius of 12 m, as seen in Fig. 4 [10].

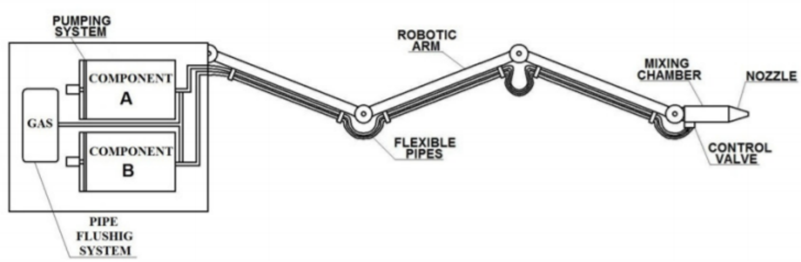

Figure 5: A diagram with the foam reservoir attached to a robotic arm and nozzle, illustrating the deployment method listed above [10].

One of the main issues with this method is the foam buildup in the nozzle after each use. This could affect the rate of foam flow, and could eventually lead to total blockage. A possible remedy to this problem is to increase the foam ejection velocity; however, too high of a velocity could generate a thrust on the debris that propels it away from the spacecraft. Another solution that seems more viable is to ventilate the ducts using an inert gas to clear any foam deposits left in the nozzle. Additionally, as with the chameleon tongue, the robotic arm requires precise data on the debris' position and velocity. The arm also has limited maneuverability in comparison to other methods, such as a satellite swarm or a foam gum dispenser.

Satellite Swarm

The satellite swarm method utilizes a constellation of satellites that are each equipped with a foam ejection nozzle. The constellation, or one of its subgroups, surrounds a large piece of debris and sprays it with foam from many points. This greatly increases the chance of total coverage of the debris. In addition, each satellite would be capable of spraying small debris by itself.

The main drawback to this method is that the proposed satellites have a low storage capacity for the components of the foam. Consequently, this system can only deorbit a small amount of debris mass unless a method for refilling is developed. Furthermore, the satellite swarm is the most expensive method as it necessitates the production of multiple separate complex bodies, unlike other methods. Finally, an area for development exists in coordination of the satellite swarm towards the goal of deorbiting debris.

Foam Gums

A reservoir, called a gum, is filled with foam components and shot onto the surface of the debris. Once on the debris, the foam components mix to create the foam which the gum then releases onto the surface. The chambers are estimated to have a volume of 10 cm^3, with 1000 L (expanded volume) of foam.

Once again, this method exists mostly in theory. There is little research in the deployment of projectiles to apply foam to orbiting bodies. Additionally, the gum must be fired from a device on the spacecraft that can track debris of different sizes, velocities, and rotations. Moreover, the momentum from the gum impacting the debris poses a potential problem. The impact itself could deorbit the debris or add/remove spin, making the debris more unpredictable overall. Finally, for very large bodies, multiple gums could be required to successfully deorbit the debris.

These are the few methods of deployment for foam from a single paper. Although there are many other method possibilities, the field requires more research into possible deployment methods, which falls outside of the scope of this paper.

2.3 Foam Static Mixing Nozzle Design

In the aforementioned paper, the suggested nozzle is specifically a static mixing nozzle. We will briefly describe how this nozzle works, as the nozzle is incorporated into many other deployment methods. In a static mixing nozzle, two liquids are forced through a long nozzle with many scaffolds obstructing flow inside the nozzle. As seen in Fig. 6 below, these scaffolds force the liquids to combine through static means, or without the addition of energy or motion. In this way, two liquids can be easily mixed by forcing them through the nozzle with high pressure at one end. Due to the simple nature and implementability in space, static mixing nozzles are the optimal choice for a nozzle design. The exact shape of the nozzle tip, placement of scaffolds inside, as well as length of the nozzle, are all quantities that must be considered in nozzle design.

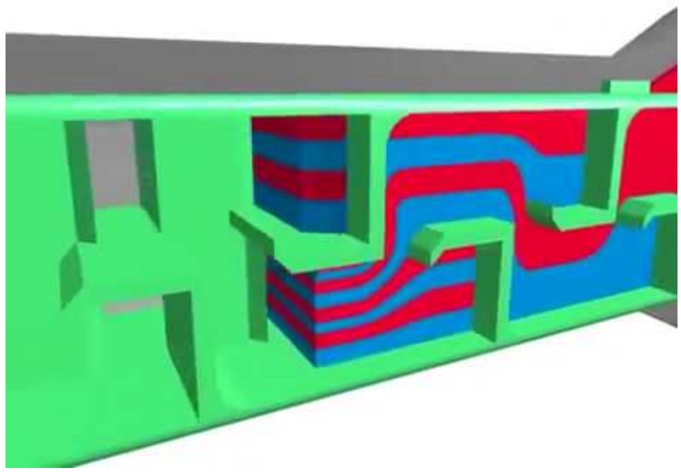

Figure 6: A diagram depicting the mechanisms behind a static mixing nozzle. The two reservoirs of red and blue fluid are mixed statically without the addition of energy or motion [11].

2.4 Types of Foams

The possible candidates for the foam can be separated into two categories related to the cell structure of the foam determined within the paper by Andrenucci et al. in 2011:

Closed-Cell Foams

Types of foam in which an insulating gas is retained within the cells during decomposition. This makes closed-cell foams great insulators with very low permeability and good water resistance.

Open-Cell Foams

Types of foam in which the cell structure is not closed and an insulating gas is not trapped within the foam during decomposition. This makes open-cell foams less dense than closed-cell foams. Open-cell foams however are much more permeable and worse insulators than closed-cell foams.

These categories are useful for organization of foam types by physical structure; however, each individual type of foam has unique characteristics that are not described by the two categories above. Below, additional types of chemistry are listed along with a brief description of their general chemical properties:

Glass Foams

Glass foams, a type of closed-cell foam, are made from molten glass or sintered — meaning compaction by heat and pressure until just before liquefaction — glass particles. They are generally more brittle than other foams. The longevity of the structural properties makes them suitable for insulation applications. The initial state of the glass used determines the need for a foaming agent; for instance, sintered glass particles will require a foaming agent in foam production. When the foam is made, the foaming agent decomposes into a gas that is trapped within the melted glass material so long as the viscosity of the fluid is sufficient [10]. It is noted that the temperature of the reaction is critical; if the temperature becomes too high, the gas bubbles will rise excessively causing a collapse of the overall structure of the material [10]. In a patent developed by Solomon et al. in 1992, the particle size of the foaming agent will affect the foam's cell dimension and thus the density [12]. A lower density results in a lower thermal conductivity, while a smaller cell dimension results in higher compressive strength [10]. The associated brittleness of glass foams is unsuitable for application to space debris removal.

Ceramic Foams

Ceramic foams are an incredibly flexible category of foams, including both open and closed-cell foams, with a wide range of adjustable material properties, such as electrical resistance. Because of this flexibility, ceramic foams have a large number of applications on Earth including thermal protection systems and filters. In 2005, Biasetto discussed three techniques for developing ceramic foams: development by 1) filling the cellular structure of a polymeric foam with a ceramic suspension and then removing the polymeric foam, 2) preparing a continuous ceramic matrix and then burning out sections to create the intended porosity, or 3) direct foaming, which utilizes a blowing agent to generate a ceramic foam mixture [13]. All three of these techniques would be extremely difficult and expensive to perform in space with current technologies, making ceramic foams a poor choice for debris removal.

Metallic Foams:

Metallic foams can be either open cell or closed cell, depending on the manufacturing process [14]. Metallic foams are essentially a metallic structure with gaseous pores throughout and primarily retain the physical characteristics of the original metal. In general, the pores lower the density of the structure, but it varies based on the base metal's mass and the percent volume of the pores. The uses of metallic foams can vary depending on the base metal chosen, although they are most commonly used in structural applications. It should be noted that the production of metallic foams requires either a metal in its liquid state or powdered metal heated to just below the melting point to achieve the foaming process. Heating a metal to its melting point requires a large amount of energy, so applying it to the topic of deorbiting space junk means the satellite either needs to be very large to carry the premade foam, or have access to a large enough energy supply to produce the foam in orbit. Both of these are unrealistic, making metallic foam a poor choice for this application.

Polymeric Foams:

Polymeric foams encompass a wide range of polymers, including polyurethane, polyethylene, polystyrene, and polyvinyl chloride (PVC). In general, compared to other foam types, polymeric foams are less expensive and more widely available while still maintaining desirable properties. Depending on the exact composition of constituent ingredients such as foaming agents, properties like density, flexibility, and material strength vary widely, even between foams of similar polymers. Such flexibility of options in polymeric foams enable them to be used in a variety of purposes, a clear advantage compared to the previously discussed foam chemistries.

Additionally, composite foams expand upon previously discussed foam types by introducing an additional hollow phase or solid phase to the foam material, allowing for the enhancement of specific properties such as improved strength/rigidity. For the purpose of this research, the foam materials are classified to be biphasic (consisting of two phases of matter) and are defined by some firm structure surrounding hollow regions, or gas bubbles, within the material [10]. Table 1 below summarizes the general physical properties of closed and open cell foams:

Closed-cell	Open-cell
Low vapour permeability	High vapour permeability
Good water insulating	Good sound insulating
Medium density	Low density
High strength and rigidity	Low strength and rigidity

Table 1: Comparison of open-cell and closed-cell foams based on physical characteristics [10].

Based on the summarizations above, open-cell foams are generally lighter in mass than closed-cell foams which correspond to the lower density associated with open-cell foams. However, the lower density implies a greater yield for the volume of foam produced for each unit of mass, which is important in the expansion of the foam around a material. Under the assumption that the foam is to be deployed in near-vacuum when applied in the removal process, the comparison of the vapor permeability of each type of foam would only be factored as the debris enters the atmosphere upon removal, however in near vacuum with miniscule amounts of vapors present, the comparison may not be needed for these conditions.

Overall, the previous study by Andrenucci et al. chooses to focus on the application of open-cell foams in the removal process. Our research can investigate the expansion properties of each type of foam under standard atmospheric conditions as well as near-vacuum conditions similar to those of objects in orbit around Earth to further focus on what type of foam to baseline in application.

2.5 Foam Expansion Properties

Based on previous work by Bruchon and Copez, an expansion model was derived from the Rayleigh-Plesset equation and rearranged to solve for the expansion of bubble radius [16]. The study done by Andrenucci et al. implements this foam expansion model in a scenario that is subject to low pressure conditions, to simulate the effect that space will have on the foam expansion process. The study uses the theoretical model derived, assumptions on the gas created during expansion, ESPAK 90 polyurethane resin as the polymeric foam, and other physical atmospheric quantities such as pressure, density, and viscosity to create its simulations.

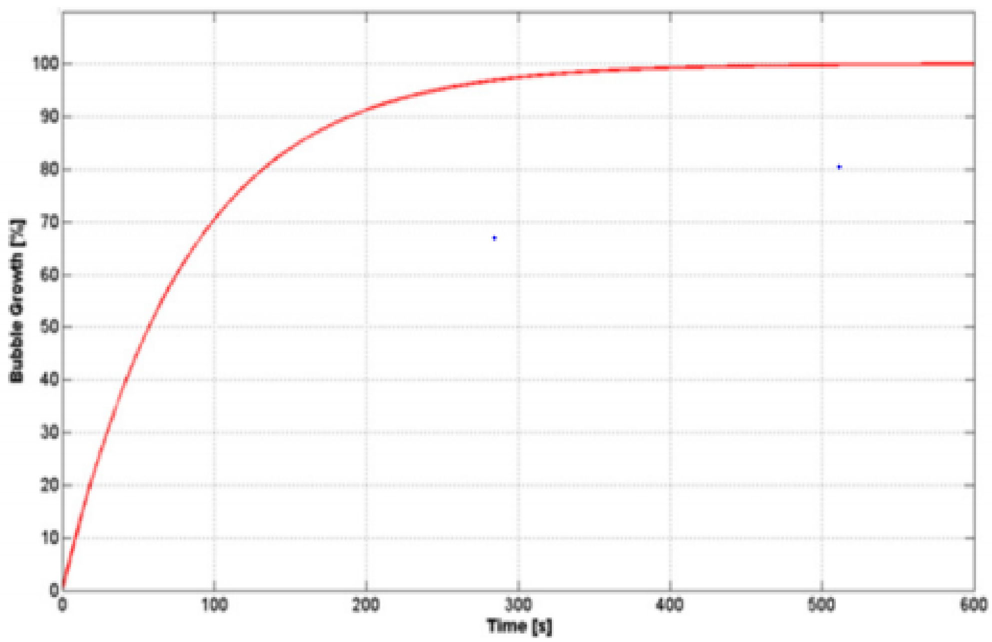

Figure 7: Expansion of foam bubble over time [10].

Although the expansion time, reaction time, and final radius of the foam have been accredited in another study, there has been no testing to date on the expansion of foam in upper-atmospheric conditions. However, both studies have verified that the foam takes under a minute to expand fully, with a reaction time around 0.2 s.

One important aspect is the viscosity and how this affects the process time of foam expansion. According to the original derived expansion model, there are no significant effects on the volume of the final foam expansion caused by viscosity. However, in low pressure conditions, viscosity becomes a factor that greatly influences the reaction time of the foam. This is likely because viscosity influences the ability of the foam to expand under atmospheric pressure and therefore a greater viscosity leads to a longer process time.

Another significant factor in the foam expansion model is its dependence on ambient pressure, the pressure of the surrounding medium. As pressure decreases, the final volume and reaction time increase, and this relation can be examined in Fig. 8.

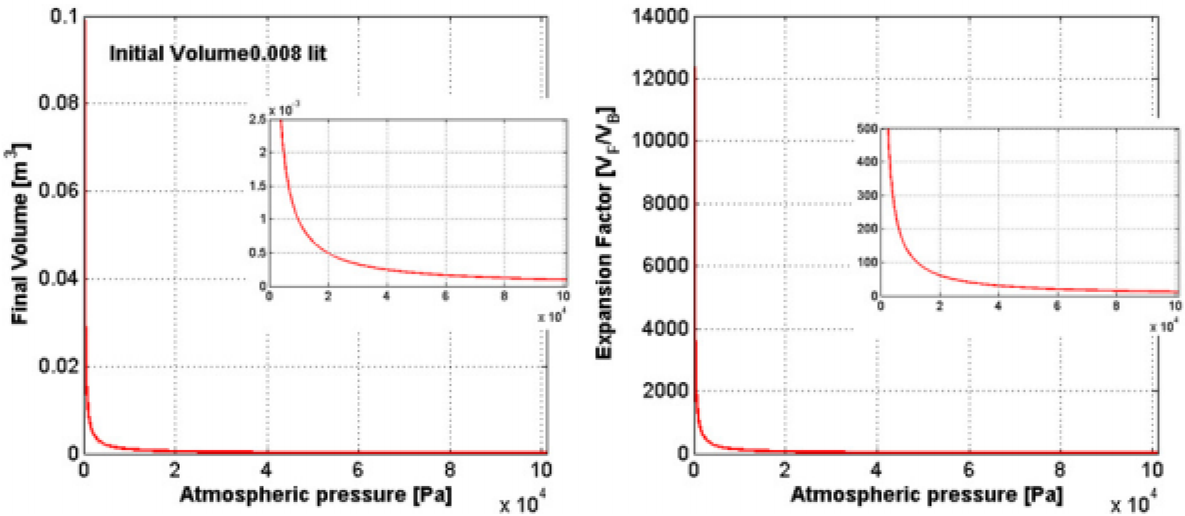

Figure 8: Expansion Factor in terms of final volume and pressure [10].

2.6 Review Conclusion

From above, we discussed previous work on foam in debris removal. It has been found that using foam to increase the surface area of debris is a feasible solution for debris removal. There are numerous reasonable techniques for foam deployment, including placing a mixing chamber that releases foam onto debris, and spraying the debris with foam ejected from nozzles. The different cell structures, and materials for foams were discussed and their benefits were established. Polymeric foams were found to be the best for the removal of debris due to their density and expansion properties. This suggests further research into the exact expansion properties of polymeric foams in the upper atmosphere.

3 METHODOLOGY

3.1 Final System Design

The design for the testing apparatus is shown in Figure 9 below. The reagents are initially loaded into the two syringes at the top of the vacuum chamber, which feed through two manual stopcock valves, through the top plate, and into the static mixer. With two separate lines for Reagents A and B of the foam, the mixing is delayed until the reagents enter the vacuum chamber. After passing through the static mixing nozzle, the two reagents are mixed by the partitions located inside the mixing nozzle itself, eliminating the need for active mixing. The choice of a passive mixer was made to avoid the complications of including an active mixer in the vacuum chamber. Once mixed, the liquid foam is ejected into a measuring cup and allowed to fully expand over the course of ten minutes.

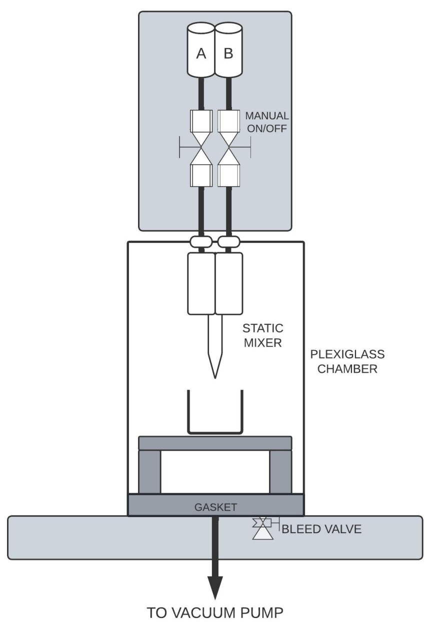

Figure 9: Block diagram of the test apparatus.

In the system described, almost every part of the design is replaceable. After extensive testing of various cleaning methods, including the use of acetone through reagent feeds, it was determined that the diameter of the flow path was too small to allow for effective cleaning. After only a few tests, the valves, tubes, or static mixer would become clogged with excess reagent or foam. To avoid these issues, every part in the foam feed is able to be replaced without impacting the consistency of testing and data collection. During testing, the entire feed system is evaluated for blockages after each run, and replaced following two to three runs to avoid accumulation.

The system design is kept simple to avoid sources of error. As discussed below, the iterative process for data collection is lengthy, and initial complex system designs had many points of air leaks, inconsistent flow speeds, and other prohibitive issues. The decision to keep the design simple was made through an extensive iterative process, as discussed below.

3.2 Vacuum Chamber Design

Federico et. al. designed an apparatus to test foam mixing in a microgravity and low pressure environment. The system was integrated into the Rexus 12 sounding rocket, but unfortunately the rocket malfunctioned and never reached orbit. In order to increase the repeatability of tests and to reduce risk, a custom vacuum chamber was designed instead. The system cannot replicate a microgravity environment, but it can replicate to a degree the low pressure environments of LEO. The final design of the chamber consisted of a custom acrylic cylinder and baseplate, and was designed to match the vertical top-down deployment method. The custom baseplate had two holes drilled into it, which allowed for the valves to be mounted on top of the cylinder. This minimized the distance between the syringes and the static mixing nozzle. This minimal distance helped to minimize the issue of the difference in viscosity of the reagents.

The baseplate and cylinder both needed to be able to withstand the stress of the vacuum. Let b be the radius of the cylinder, t be the thickness, q is the external pressure acting on the cylinder, and σ_0 the tensile yield strength of the material. Figure 10 shows the relationship between the ratio of b/t and q/σ_0, where if the value of $(b/t,\ q/\sigma_0)$ falls above the curve, the cylinder will fail (Dell'Aqua and Luzzi, 2005). The tensile yield stress of acrylic at room temperature is 69 MPa [17]. The external pressure is one atmosphere, or 101 kPa. In order to provide enough room for the test apparatus, the diameter of the cylinder of our vacuum chamber is 12 inches, or 0.304 meters. In order to maintain a safety factor of 2, a thickness of 0.25 inches was chosen.

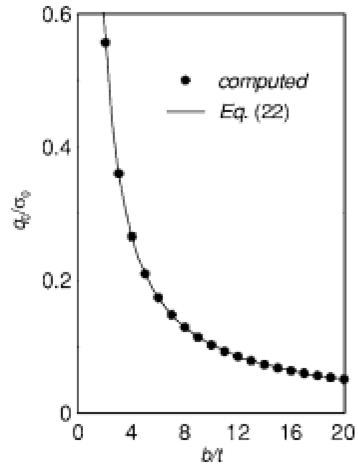

Figure 10: Limit External Pressure of a Cylindrical Vacuum Chamber.

The electronic valves' interior bore size limited reagent flow and caused clogging, so manual stopcock valves were used as a replacement. After extensive iteration, the system reached a "successful" state and data collection could proceed. The next section explains in detail the iterative process the design of the system went through.

3.3 System Validation / Iteration

In validating the system design, there were two main criteria that constituted a successful system and mixing test: (1) the ability for foam to enter the vacuum chamber as a well-mixed fluid, and (2) the ability for the tests to be repeated with the same procedure. In designing the system described above, there were many failed designs that were unable to meet either or both of these criteria. Designs with the reagent feeds below the vacuum chamber led to poorly mixed foam solutions, and those that used electrically-actuated valves above the chamber were unable to repeat tests extensively due to clogging and ineffective cleaning. In addressing some of these issues, the initial vacuum design had to be reworked, as discussed in the above section (3.2). By limiting the size of the vacuum chamber, as well as mounting the deployment system above the chamber, the foam reagents were deployed at lower pressures and mixed more easily.

3.4 Experimental Procedure and Data Collection

To validate previous studies' models on spray foam in vacuum, 5 mL of each part of a two-part polyurethane foam manufactured by Composite Envisions, according to the manufacturer-recommended 1:1 ratio, were loaded into syringes above the two closed stopcock valves. The system was then pumped down to vacuum. The strength of vacuum was determined by allowing the vacuum to come to a natural equilibrium, or in cases where the vacuum strength was abnormally low, until the pressure was under 100 mBar. Once the resting pressure is reached, the valves are opened and the syringes are pulled by the vacuum to deploy the foam into a clear beaker with volume demarcations. The foam is allowed to expand for approximately 10 minutes, or until the foam reaches a peak expansion. The total volume of the foam is recorded, along with the pressure of the vacuum, and the vacuum is then vented. The valves and tubes above the baseplate are cleaned with water or replaced if they become clogged, and the static mixer is replaced with a fresh mixer after every test.

3.5 Additional Testing

After preliminary data collection, the observation was made that at low enough pressures, the foam would continuously collapse while expanding, causing the final volume to be much lower than anticipated. Although the cause of this phenomenon is unknown, it was observed that by varying the mixture ratio of reagents, the collapsing could be avoided. Mixture ratios of 1:2 and 2:1 were tested, and it was found that by using a ratio of 1:2 (2.5 mL of Reagent A and 5 mL of Reagent B), the collapse was avoided completely. However, due to time constraints, the testing could not be redone with this new mixture ratio. Further research into this collapse phenomenon and varying mixture ratios must be done to determine if they significantly affect the viability of foam-based remediation.

4 RESULTS

4.1 Raw Data

In total, 21 tests were accumulated for foam mixture in our vacuum system with all measurements. The measured expansion factors of the foam as pressure was varied lied in a range of 0 to 60. The 21 tests include a combination of tests deemed successes and failures, which were determined by either the collapse of the foam, or due to failures in the deployment or mixing stages. Table 2 below summarizes the results of the combined successes and failures:

Pressure (millibar)	Reagent A Volume (mL)	Reagent B Volume (mL)	Total Expanded Volume (mL)	Expansion Ratio
141.0 ± 0.001	3.5 ± 0.2	3.5 ± 0.2	380.0 ± 29.5	54.3 ± 4.8
300.0 ± 0.001	3.0 ± 0.2	3.0 ± 0.2	100.0 ± 20.0	16.7 ± 3.4
280.0 ± 0.001	5.0 ± 0.2	5.0 ± 0.2	400.0 ± 30.0	40.0 ± 3.2
170.0 ± 0.001	3.0 ± 0.2	3.0 ± 0.2	20.0 ± 14.5	3.3 ± 2.4
120.0 ± 0.001	3.0 ± 0.2	3.0 ± 0.2	200.0 ± 24.1	33.3 ± 4.2
40.0 ± 0.001	5.0 ± 0.2	5.0 ± 0.2	50.0 ± 17.1	5.0 ± 1.7
180.0 ± 0.001	5.0 ± 0.2	5.0 ± 0.2	350.0 ± 28.7	35.0 ± 3.0
100.0 ± 0.001	5.0 ± 0.2	5.0 ± 0.2	450.0 ± 31.2	45.0 ± 3.4
213.0 ± 0.001	5.0 ± 0.2	5.0 ± 0.2	375.0 ± 29.4	37.5 ± 3.1
370.0 ± 0.001	5.0 ± 0.2	5.0 ± 0.2	350.0 ± 28.7	35.0 ± 3.0
70.0 ± 0.001	5.0 ± 0.2	5.0 ± 0.2	400.0 ± 30.0	40.0 ± 3.2
15.0 ± 0.001	5.0 ± 0.2	5.0 ± 0.2	20.0 ± 14.5	2.0 ± 1.4
112.5 ± 0.001	5.0 ± 0.2	5.0 ± 0.2	500.0 ± 32.4	50.0 ± 3.5
84.1 ± 0.001	5.0 ± 0.2	5.0 ± 0.2	10.0 ± 13.2	1.0 ± 1.3
40.0 ± 0.001	5.0 ± 0.2	5.0 ± 0.2	50.0 ± 17.1	5.0 ± 1.7
140.0 ± 0.001	5.0 ± 0.2	5.0 ± 0.2	400.0 ± 30.0	40.0 ± 3.2
97.4 ± 0.001	5.0 ± 0.2	5.0 ± 0.2	350.0 ± 28.7	35.0 ± 3.0
79.6 ± 0.001	5.0 ± 0.2	5.0 ± 0.2	300.0 ± 27.3	30.0 ± 2.9
70.0 ± 0.001	5.0 ± 0.2	5.0 ± 0.2	250.0 ± 25.8	25.0 ± 2.7
80.0 ± 0.001	5.0 ± 0.2	2.5 ± 0.2	100.0 ± 20.0	13.3 ± 2.7
60.0 ± 0.001	2.5 ± 0.2	5.0 ± 0.2	450.0 ± 31.2	60.0 ± 4.7

Table 2: Foam volume expansion ratios for changing pressure

The measured expansion factors for each test listed in Table 2 were calculated by taking the final expanded volume and dividing it by the total initial reagent volume, which was a sum of the initial volume of each reagent. In order to conduct analysis on our data and complete a comparison to the model of polyurethane foam expansion [10], the tests determined to be failures were removed from the data set analyzed. Additionally, the tests with unequal initial reagent volume were also removed from the final data set, as the model used assumes a complete reaction between both components. Table 3 below lists the resulting successful tests, of which 12 remained:

Pressure (millibar)	Total Expanded Volume (mL)	Total Initial Volume (mL)	Expansion Ratio
141.0 ± 1.0E-3	380.0 ± 29.5	7.0 ± 0.3	54.3 ± 4.8
280.0 ± 1.0E-3	400.0 ± 30.0	10.0 ± 0.3	40.0 ± 3.2
180.0 ± 1.0E-3	350.0 ± 28.7	10.0 ± 0.3	35.0 ± 3.0
100.0 ± 1.0E-3	450.0 ± 31.2	10.0 ± 0.3	45.0 ± 3.4
213.0 ± 1.0E-3	375.0 ± 29.4	10.0 ± 0.3	37.5 ± 3.1
370.0 ± 1.0E-3	350.0 ± 28.7	10.0 ± 0.3	35.0 ± 3.0
70.0 ± 1.0E-3	400.0 ± 30.0	10.0 ± 0.3	40.0 ± 3.2
112.5 ± 1.0E-3	500.0 ± 32.4	10.0 ± 0.3	50.0 ± 3.5
140.0 ± 1.0E-3	400.0 ± 30.0	10.0 ± 0.3	40.0 ± 3.2
97.4 ± 1.0E-3	350.0 ± 28.7	10.0 ± 0.3	35.0 ± 3.0
79.6 ± 1.0E-3	300.0 ± 27.3	10.0 ± 0.3	30.0 ± 2.9
70.0 ± 1.0E-3	250.0 ± 25.8	10.0 ± 0.3	25.0 ± 2.7

Table 3: Foam volume expansion ratios for changing pressure, successful tests

4.2 Analytical Results

To compare the successful tests collected against the polyurethane foam expansion model [10], a chi-squared goodness of fit test will be used to quantify how well our expansion factors compare with the expected factors predicted by the model. The pressure and volume units used by the model are in Pascals and cubic meters, respectively, thus each measured quantity was converted as needed for fitting.

In order to implement the model, the same assumptions made by Andrenucci et. al. [10] were made, as well as similar constants used. The gas generated in the foaming reaction by the two reagents is carbon dioxide (CO_2) gas, which has a gas constant of $R_G = 188.9233\, m^2/Ks^2$. Using this constant, along with the standard atmospheric pressure of 101325 Pa, and an assumed room-temperature of 293 K, the density of the CO_2 gas released is about $1.8\, kg/m^3$. The relative densities of reagent A and B are provided to be $1.24\, g/mL$ and $1.12\, g/mL$, respectively, thus combining to give an overall relative density of $\rho_{reagents} = 1.18\, g/mL$ for the combined reagent mixture immediately before foaming. Based on the expansion factor for each measurement, the amount of initial mass of reagent transformed into gas varies for each test. The initial volume of gas thus varies based on the varying initial mass of CO_2 gas present, and can be used to get the initial CO_2 gas bubble radius.

That initial CO_2 gas bubble radius is determined by the initial volume of CO_2 gas generated at the start of the reaction, and is dependent on how much initial reagent mass is converted into CO_2 gas. The percentage of reagent mass converted into CO_2 gas is found by determining the initial mass of the reagents and the final mass of the CO_2 gas as follows:

$$m_{gas} = \rho_{gas} V_{total, final} \quad (1),$$

$$m_{reagents} = \rho_{reagents} V_{total, initial} \quad (2),$$

After taking a ratio of the resulting CO_2 mass to the initial reagent mixture mass, the % of reagent converted into gas by the reaction is then factored into determining the initial CO_2 gas bubble radius. This ratio is quantified by the “Mass Conversion Factor” in Table 4 below. From this conversion factor, at the initial point of reaction between the reagents, the estimated initial volume of CO_2 gas is found by:

$$V_i = \frac{\rho_{reagents} V_{total,\,initial}}{\rho_{gas}} * M_{conversion} \quad (3),$$

with V_i being the initial CO_2 gas volume. Since there is no CO_2 gas present prior to reaction between the reagents, this initial volume is estimated to be shortly after the chemical reaction begins.

The change in CO_2 gas bubble radius is modeled by the following relation:

$$R(t) = R_{bubble}[(1 - \frac{P_{bubble}}{P_{chamber}})e^{-\frac{3P_{chamber}}{4\mu}t} + \frac{P_{bubble}}{P_{chamber}}]^{1/3} \quad (4),$$

with μ being the viscosity of the foam, R_{bubble} being the initial CO_2 gas bubble radius, P_{bubble} being the initial pressure of the CO_2 gas at the start of mixing, and $P_{chamber}$ being the pressure of the environment surrounding the foam reaction. The maximum change in radius of a singular CO_2 gas bubble during expansion can be found by taking the difference between the radial expansion for infinite time allowed, $R(\infty)$, and the initial gas bubble radius at t = 0:

$$\Delta R = R(\infty) - R(0) = R_{bubble}[(\frac{P_{bubble}}{P_{chamber}})^{1/3} - 1] \quad (5),$$

The initial pressure of the CO_2 gas is chosen to be approximately atmospheric pressure, as the two reagents begin mixing and reacting within the static mixing chamber while being forced into the chamber by atmospheric pressure. The initial gas bubble radius is found through the assumption that each gas bubble is essentially spherical, and thus the change in volume and the expansion factor can then be found by:

$$\Delta V = \frac{4}{3}\pi(\Delta R)^3 \qquad f = \frac{V_f}{V_i} = \frac{V_i + \Delta V}{V_i} \quad (6).$$

One item to note is that the model predicts nearly no expansion in atmospheric pressure conditions, however the model used the assumption from previous research that polyurethane foams have an expansion factor between 10 - 16 at atmospheric pressure. To account for this difference, a factor of 14 was added to the final expansion factor. Table 4 and Figure 11 below summarize the results of applying the model to the polyurethane foam used.

Mass Conversion Factor (%)	Initial Gas Volume (m^3)	Initial Bubble Radius (m)	Change in Radius (m)	Change in Volume (m^3)	Theoretical Expansion Factor
8.4 ± 0.7	3.8E-4 ± 3.7E-5	4.5E-2 ± 1.4E-3	9.2E-2 ± 1.3E-3	3.2E-3 ± 3.4E-5	23.5 ± 9.7E-2
6.2 ± 0.5	4.0E-4 ± 3.4E-5	4.6E-2 ± 1.3E-3	7.4E-2 ± 6.9E-4	1.7E-3 ± 1.8E-5	19.3 ± 8.5E-2
5.4 ± 0.5	3.5E-4 ± 3.2E-5	4.4E-2 ± 1.3E-3	8.2E-2 ± 1.0E-3	2.3E-3 ± 2.5E-5	21.7 ± 9.1E-2
7.0 ± 0.5	4.5E-4 ± 3.6E-5	4.8E-2 ± 1.3E-3	1.1E-1 ± 1.5E-3	5.4E-3 ± 4.2E-5	27.0 ± 8.0E-2
5.8 ± 0.5	3.8E-4 ± 3.3E-5	4.5E-2 ± 1.3E-3	8.0E-2 ± 8.9E-4	2.1E-3 ± 2.2E-5	20.6 ± 8.8E-2
5.4 ± 0.5	3.5E-4 ± 3.2E-5	4.4E-2 ± 1.3E-3	6.5E-2 ± 5.3E-4	1.1E-3 ± 1.3E-5	18.2 ± 9.1E-2
6.2 ± 0.5	4.0E-4 ± 3.4E-5	4.6E-2 ± 1.3E-3	1.2E-1 ± 1.9E-3	6.9E-3 ± 4.9E-5	32.1 ± 8.6E-2
7.8 ± 0.5	5.0E-4 ± 3.8E-5	4.9E-2 ± 1.2E-3	1.1E-1 ± 1.3E-3	5.3E-3 ± 4.1E-5	25.7 ± 7.6E-2
6.2 ± 0.5	4.0E-4 ± 3.4E-5	4.6E-2 ± 1.3E-3	9.4E-2 ± 1.2E-3	3.4E-3 ± 3.2E-5	23.6 ± 8.5E-2
5.4 ± 0.5	3.5E-4 ± 3.2E-5	4.4E-2 ± 1.3E-3	1.0E-1 ± 1.6E-3	4.3E-3 ± 3.8E-5	27.3 ± 9.2E-2
4.7 ± 0.4	3.0E-4 ± 3.0E-5	4.2E-2 ± 1.4E-3	1.0E-1 ± 1.8E-3	4.5E-3 ± 4.0E-5	30.1 ± 1.0E-1
3.9 ± 0.4	2.5E-4 ± 2.8E-5	3.9E-2 ± 1.4E-3	1.0E-1 ± 2.1E-3	4.3E-3 ± 4.0E-5	32.1 ± 1.1E-1

Table 4: Foam expansion model per test conditions, adjusting factor used to determine initial amount of CO_2 gas

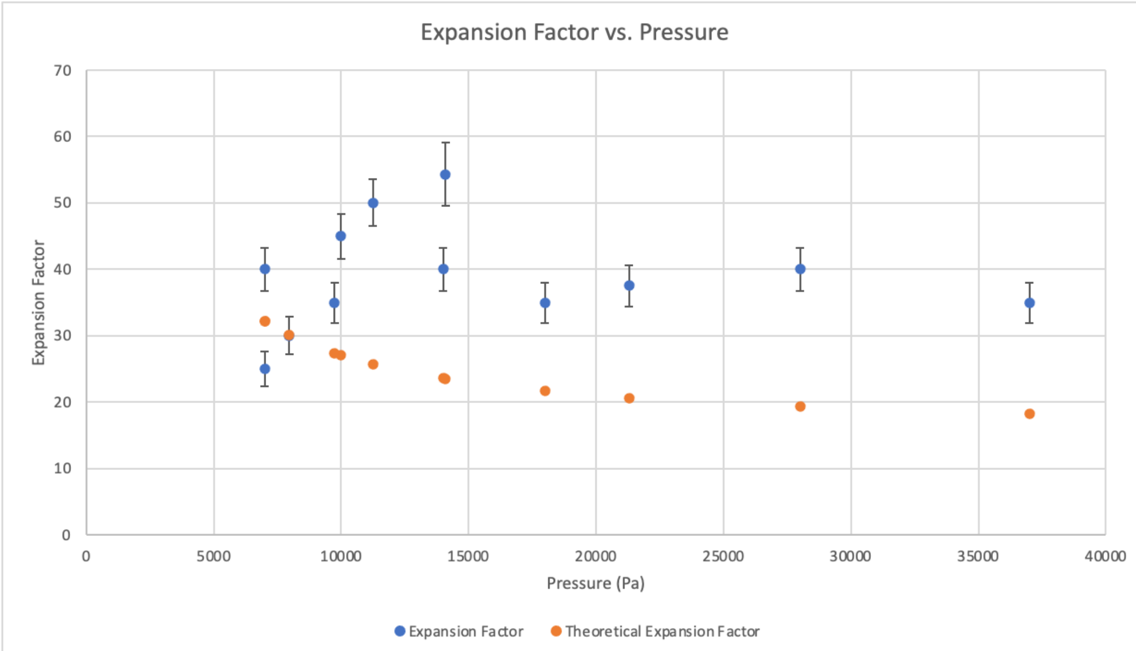

Figure 11: Plot of foam expansion factor vs. pressure, measured and theoretical values.

To quantify the difference between the measured expansion factors and those predicted by the model, a total χ^2 value of 152.1 was found which corresponds to a reduced χ^2_{ν} value of 12.7. Since the atmospheric pressure level, room-temperature, and relative densities of each reagent do not affect the expansion factor of the predicted model, for a χ^2 value of 152.1 with 11 degrees of freedom, the resulting p-value is on the order of 2E-26, and would thus result in a rejection of the null hypothesis which assumes the model is a valid model for foam expansion.

5 DISCUSSION

5.1 Findings from Data Analysis

From the plot in Figure 11, visually there is a clear difference between the expansion factors predicted by the foam expansion model and our measured values. Only a singular point is in agreement with the model within uncertainties, and thus this leads to an extremely high reduced χ^2_{ν} of 12.7. The p-value of 2E-26 resulting from the goodness of fit test suggests significant rejection of the null hypothesis at any level. However, despite the significant difference, the measured expansion factors appear to follow a relatively flat or slightly increasing trend as pressure decreases. The foam expansion model also predicts this behavior, with the expansion factor scaling as $(Pressure)^{-1}$. For pressures in this range, the model does not predict incredibly large increases in expansion factor. Thus, the data behaves similarly to the model, however that does not resolve the significantly large expansion factors measured.

The model assumes that the percentage of initial reagent mixture mass being converted into CO_2 gas is consistent, however failure to properly mix the reagents together into this initial mixture may alter that percentage, thus resulting in less CO_2 gas produced by the reaction. The result would be a decrease in expansion factor, however in this case a lower expansion factor would further align the model and the measurements, as opposed to causing a deviation away from the model. The atmospheric pressure level, room temperature, and reagent densities did not affect expansion factors when changed, thus these factors did not deviate the measurements from the model.

5.2 Sources of Error

During our data collection, it was apparent that some of our results were subject to sources of error and uncertainty. In our particular case, our system was not automated, and therefore, while we were conducting experiments, we introduced variables of human error into the equation. The most common example was not releasing both of the foams into the static mixing chamber simultaneously, resulting in inadequate mixing that often led to a lack of expansion. During the experiments in which our ratio was 1:1, this was not as big of an issue, but we wanted to test different ratios of our foam reagents to see whether certain factors within the foam (viscosity, density, etc) would affect its expansion. Therefore, we adjusted our ratios to 1:2 and 2:1 (5 mL of reagent A vs 2.5 mL of reagent B, for example), which meant that the person deploying the reagent with more volume had to deploy at a faster rate than the person deploying the reagent with less volume. This led to scenarios in which the timing of the experiment was not precise, which is a critical factor for achieving the ideal foam expansion ratio.

Additionally, precision errors in our equipment affected our physical measurements. The syringes that we used to measure the initial volume of and deploy the foam reagents were capable of measuring volume at a resolution of 0.2 mL, and thus leading to errors on the initial volume on that order. Our measuring cups used to determine final expanded volume also had precision limitations, being capable of measuring volume at a resolution of 10 mL. As observed during testing, due to the foam not uniformly filling the volume of the cup as it expanded, a larger uncertainty would be required for each expanded volume. For that reason, the uncertainty on expanded volume was adjusted to the resolution summed with the square root of the expanded volume, as larger expansion would lead to less uniform filling of the cup. The pressure gauge used to measure pressure in the vacuum system had a resolution on the order of 0.001 millibar, thus leading to pressure uncertainties on that order. The combination of lack of precision between the timing and the initial volume of the mixture caused our reactions to fall under expectations.

Another issue our team ran into that we believe could have contributed to our experiments were the air bubbles that accumulated when measuring our foam reagents using the syringe. Research suggests that there is a strong dependance of the foam expansion process from the external pressure and "as pressure decreases…. the final volume and the reaction time increases". However, air bubbles introduce an increase in external pressure while the foam is being deployed into the static mixing chamber. Experiments from previous papers also showed that introducing bubbles into the mixture created complexity based on how the bubbles reacted with each other, causing the bounding surfaces to form abnormal shapes where the increase in surface tension caused our reactions to collapse and lose a significant portion of the expected expansion ratio.

6 CONCLUSION

Space debris management continues to be a relevant issue of discussion as thousands of satellites enter low Earth orbit each year. Of various removal systems that have been proposed and being developed, foam-based removal showed promise for its adaptability to a range of debris sizes and its relative operational simplicity. From research and testing, a polyurethane foam is likely the simplest and least expensive option to get expansion and adhesion in space – however, its deployment presents unique challenges with vacuum and microgravity. This paper explored behavior of the former environmental factor, testing the expansion of a commercially available polyurethane foam under low-pressure environments to quantify the expansion factor as a function of air pressure. Testing found that the foam expansion exceeds predictions down to an air pressure of around 70 millibar, where the foam would tend to structurally collapse under its own weight. During testing, problems with foam reagent deployment timing, adhesion, as well as structural integrity upon deployment were encountered and recorded. In particular, reagents sticking to the sides of the deployment system tubes Full rectification of these problems could be focuses of further research, which would be incremental towards the verification of foam deployment viability in vacuum. In addition, a microgravity environment may present different structural behavior than what was encountered in this testing, where the foam may not collapse due to its low density when deploying in vacuum. All of these factors will need to be evaluated to show that foam as a space debris removal method will actually function in its intended working environment, prior to evaluating its deorbiting performance.

7 APPENDICES

7.1 Appendix A: Equity — Impact Analysis

Space debris removal is a specialized field that has not had a lot of research done into how it could have an equitable impact on the affected populations. For that reason, we did not place a strong emphasis on that aspect of our research in our literature review. However, there are ways that this research could apply in that scope.

A lot of the satellites that currently exist in LEO are useful in day to day life, whether they be weather observing satellites, communication satellites used in phones, or satellites used in radios. If the continuing space debris problem worsens, it could lead to the disruption of these services for certain populations; populations that could very much rely on these services, and have limited access to alternative solutions. As an example, without satellites to monitor weather, people may find it a lot more difficult to prepare for predictable natural disasters like incoming hurricanes. In our equity-impact report, we will focus on aspects such as the one described.

It was also our intention to cite sources from a diverse collection of researchers. However, we ran into a problem with this because of the novelty of foam-based remediation methods. There is not a lot of existing research in the field of space debris, and even less so that focuses on foam methods. For this reason we have decided we may not be able to address citation bias as we originally intended within our paper.

7.2 *Appendix B: Project Timeline*

<u>Sophomore Year (2020–2021)</u>

FALL:

- Complete project proposal.
- Design and present preliminary testing procedures.
- Select and purchase the initial set of foams.

SPRING:

- Test viability of foams for intended testing.
- Begin design of static mixing nozzles.
- Flesh out testing procedures, and test chamber design.
- Decide on final candidates for foam procedures.

<u>Junior Year (2021–2022)</u>

SUMMER:

- Finalize testing designs, and purchase any components not already obtained.
- Create timeline for testing procedures for upcoming year.

FALL:

- Run prepared tests and begin collecting data.
- Create models based on experimental data.
- Prepare for the Do Good Showcase.

SPRING:

- Continue to iterate on nozzle design.
- Streamline tests for consistent foaming data.
- Develop the results from the tests.

<u>Senior Year (2022–2023)</u>

SUMMER:

- Continue data collection if needed.
- Wrap up research and continue data analysis.
- Plan schedule for thesis completion.
- Find research conferences to attend.

FALL:

- Work on thesis according to the determined schedule.
- Collect any final data needed for the thesis.
- Plan for research conferences.

SPRING:

- Complete the thesis and present at thesis defense.

7.3 *Appendix C: Budget*

Component	Unit Cost	Quantity	Total
Vacuum Chamber	$0.00*	1	$0.00
Solenoid Valves	$50.00	4	$200.00
Manual Valves	$15.00	10	$150.00
Graduated Cylinder	$8.00	1	$8.00
Foam Reagents	$20.00	10	$200.00
Printing Filament	$0.00**	N/A	$0.00
Hypodermic Needles	$0.70	10	$7.00
Testing Rig Frame Materials	$250	Various	$250.00
		Net Total	$815.00

*Use of vacuum chamber is free through the Space Power and Propulsion Lab

** Use of 3D printers is free under private ownership and on-campus resources

REFERENCES

1. Guerra, G., Muresan, A. C., Nordqvist, K. G., Brissaud, A., Naciri, N., & Ling LUO. (2017). Active Space Debris Removal System. INCAS Bulletin, 9(2), 97–116. https://doi-org.proxy-um.researchport.umd.edu/10.13111/2066-8201.2017.9.2.8

2. Drmola, J., & Hubik, T. (2018). Kessler Syndrome: System Dynamics Model. Space Policy, 44-45, 29–39. https://doi.org/10.1016/j.spacepol.2018.03.003

3. Leolabs, Inc. [LeoLabs_Space]. (2020, October 16). Our latest data confirms Cosmos 2004 is still intact. [Tweet]. Twitter. https://twitter.com/LeoLabs_Space

4. European Space Agency. (n.d.). Space debris by the numbers. Retrieved October 26, 2020, from http://www.esa.int/Safety_Security/Space_Debris/Space_debris_by_the_numbers

5. H. Krag, H. Klinkrad, T. Flohrer, E. Fletcher, N. Bobrinsky, The European Space Surveillance System-Required Performance and Design Concepts. 8th US/Russian Space Surveillance Workshop, Space Surveillance Detecting and Tracking Innovation, Hawaii 2010

6. Botta, E. M., Sharf, I., & Misra, A. K. (2019). Simulation of tether-nets for capture of space debris and small asteroids. Acta Astronautica, 155, 448-461. doi:10.1016/j.actaastro.2018.07.046

7. Shan, M., Guo, J., & Gill, E. (2020). An analysis of the flexibility modeling of a net for space debris removal. *Advances in Space Research*, *65*(3), 1083–1094. https://doi-org.proxy-um.researchport.umd.edu/10.1016/j.asr.2019.10.041

8. Esmiller, B., Jacquelard, C., Eckel, H., & Wnuk, E. (2014). Space debris removal by ground-based lasers: main conclusions of the European project CLEANSPACE, Appl. Opt. 53, I45-I54

9. Ebisuzaki, T., Quinn, M. N., Wada, S., Piotrowski, L. W., Takizawa, Y., Casolino, M., . . Mourou, G. (2015). Demonstration designs for the remediation of space debris from the International Space Station. Acta Astronautica, 112, 102-113.

doi:10.1016/j.actaastro.2015.03.004

10. Andrenucci, M., Pergola, P., & Ruggiero, A. (2011, February). Expanding foam application for active debris removal (Active Removal of Space Debris). ESA. https://www.esa.int/gsp/ACT/doc/ARI/ARI%20Study%20Report/ACT-RPT-MAD-ARI-10-6411-Pisa-Active_Removal_of_Space_Debris-Foam.pdf

11. MIXPAC™ Quadro mixing technology. (2017, December 21). https://www.youtube.com/watch?v=xyqnmqrI8HY.

12. Solomon, D., & Rossetti, M. (1996). *U.S. Patent No. 5516351*. Washington, DC: U.S. Patent and Trademark Office.

13. L. Biasetto, Functional Ceramic Foams from Preceramic Polymers, Ph.D. Thesis, University of Bologna, University of Padova, 2005

14. Srivastava, V., C., & Sahoo, K., L. (2007). Processing, stabilization and applications of metallic foams. Art of Science. Materials Science-Poland, 25(3), 733-753.

15. J. Bruchon, T. Coupez, A numerical strategy for the direct 3D simulation of the expansion of bubbles into a molten polymer during a foaming process. International Journal for Numerical Method in Fluids, Volume 57, Number 8, pp. 977-1003, 2008

16. Hildreth, Steven A. & Arnold, Allison. Threats to U.S. National Security Interests in Space: Orbital Debris Mitigation and Removal, report, January 8, 2014; Washington D.C.. (https://digital.library.unt.edu/ark:/67531/metadc272076/: accessed October 25, 2020), University of North Texas Libraries, UNT Digital Library, https://digital.library.unt.edu.

17. Interstate Plastics. (2012, October 15). Cast Acrylic sheet (GP) Technical information. Sacramento.